Observations of auroral broadband emissions by CLUSTER

J.-E. Wahlund,[1] A. Yilmaz,[2] M. Backrud,[1] D. Sundkvist,[1] A. Vaivads,[1] D. Winningham,[3] M. André,[1] A. Balogh,[4] J. Bonnell,[5] S. Buchert,[1] T. Carozzi,[1] N. Cornilleau,[6] M. Dunlop,[4] A. I. Eriksson,[1] A. Fazakerley,[7] G. Gustafsson,[1] M. Parrot,[8] P. Robert,[6] and A. Tjulin[1]

[1] We present the results of a study based on several events of broadband ULF/ELF emissions observed in the auroral region by the CLUSTER multi-spacecraft at distances around $4-5$ R_E. These emissions, observed below the ion plasma frequency, are similar to the broadband emissions observed at lower altitudes (800–4000 km) by rockets (e.g. AMICIST) and satellites (e.g. FREJA and FAST). As successive passages of the four CLUSTER satellites through nearly the same regions show, the intensity of the emissions depend on the thermal properties of the plasma and gradients thereof. The total Poynting flux is downward and is comparable to energy fluxes observed at lower altitudes. We believe the broadband emissions are the result of dispersed Alfvén waves (DAW), which propagates down the magnetic field lines, and emits higher frequency ion plasma wave modes. *INDEX TERMS:* 2704 Magnetospheric Physics: Auroral phenomena (2407); 2772 Magnetospheric Physics: Plasma waves and instabilities; 2712 Magnetospheric Physics: Electric fields (2411). **Citation:** Wahlund, J.-E., et al., Observations of auroral broadband emissions by CLUSTER, *Geophys. Res. Lett.*, 30(11), 1563, doi:10.1029/2002GL016335, 2003.

1. Introduction

[2] Broadband extremely low frequency (ELF) wave emissions below the ion plasma frequency have been observed by a number of spacecraft and rockets on auroral field lines [e.g., *Gurnett and Frank*, 1977; *Bonnell et al.*, 1996; *Wahlund et al.*, 1998, and references therein]. Ion-acoustic line enhancements, which could be due to the same type of broadband emissions, have been observed in EISCAT spectra during similar geophysical conditions at iono-spheric altitudes [e.g., *Wahlund et al.*, 1993]. The otherwise dominantly electric broadband emissions often include significant magnetic fluctuations at the very lowest frequencies with $\delta E/\delta B \sim V_A$ (the Alfvén velocity), which has been interpreted as the possible simultaneous presence of Alfvénic wave activity [e.g., *Chmyrev et al.*, 1989; *Boehm et al.*, 1990; *Louarn et al.*, 1994].

[1] Swedish Institute of Space Physics, Uppsala, Sweden.
[2] Çanakkale Onsekiz Mart University, Çanakkale, Turkey.
[3] Southwest Research Institute, San Antonio, USA.
[4] The Blacket Laboratory, Imperial College, London, UK.
[5] SSL, Berkeley, USA.
[6] CETP, Vélizy, France.
[7] Mullard Space Science Laboratory, London, UK.
[8] LPCE, Orléons, France.

[3] We present a first study based on 8 events from the CLUSTER multi-spacecraft mission, which aims to shed new light on the energy transport and spatial-temporal dependence of the broadband emissions. We present here only a southern auroral oval crossing on April 28, 2001. A narrow auroral arc structure, encountered within the same event, is presented in a companion letter by *Vaivads et al.* [2003], while we here focus on the wave characteristics on a larger scale. The details of the CLUSTER instrumentation can be found in *Escoubet et al.* [1997].

2. Observations of Broadband Emissions

[4] In Figure 1 we display the spin-plane **E**- and full three-dimensional **B**-field properties as measured by S/C-3. The plasma density (panel c) is inferred from the probe-to-spacecraft potential by a statistical comparison over many orbits with the plasma line emissions from the WHISPER measurements. These data are not corrected for electron temperature variations. The E-field in field-aligned co-ordinates (panel e) is derived by assuming $\boldsymbol{B}_{FGM} \cdot \boldsymbol{E} = 0$, and is used to calculate the field-aligned Poynting flux (panels f and g).

[5] A region of broadband emissions exist between 19:14–19:27 UT (panel a and b), which is clearly more electric toward larger frequencies. This is quantified in Figure 2, where the *E*- and *B*-field power spectral densities and the $\delta E/\delta B$-ratio for the "quiet" period 19:07–19:10 UT (green) and the "most active" period 19:23–19:26 UT (blue) are compared. The broadband emissions are in Figure 2 char-acterised by a one to three order of magnitude increase in electric power at all measured frequencies (panel a). The power in the magnetic component (panel b) increases below 2 Hz, and only below 0.4 Hz as much as the electric power (compare with panel c). The broadband emission enhancement is therefore electrostatic at higher frequencies and electromagnetic at lower frequencies. STAFF electric field data (not shown), which cover frequencies up to 4 kHz, show that the broadband emissions reach up to the cut-off of the auroral hiss emissions observed near 300–400 Hz. That is close to the H^+ plasma frequency.

[6] The $\delta E/\delta B$-ratio (panel c, blue) show a steady increase above 0.4 Hz, and below this frequency it is close to the Alfvén speed (V_A) between $9 \cdot 10^6 - 3 \cdot 10^7$ m/s. This kind of frequency dependence of this ratio can be interpreted as due to dispersed Alfvén waves (DAW) [*Lysak and Lotko*, 1996; *Stasiewics et al.*, 2000; *Shukla and Stenflo*, 2000], possibly the result of the Alfvén current-convective interchange mode [*Seyler and Wu*, 2001], where for $\beta = 2\mu_0 n_e k_B T_e / B_0^2 \ll 1$ the dispersion approximately becomes

$$\left(\frac{\omega}{k_\parallel V_A}\right)^2 \approx \frac{(1 + k_\perp^2 \rho_s^2)}{(1 + k_\perp^2 \lambda_e^2)} \tag{1}$$
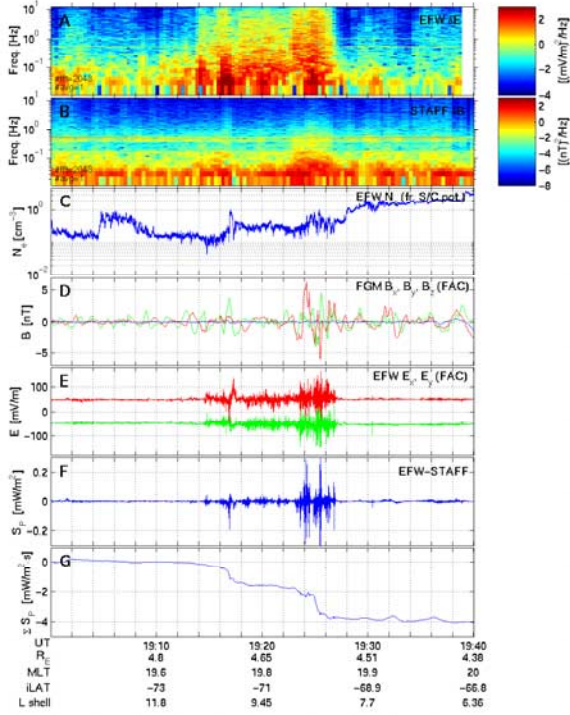
Figure 1. The E- and B-field properties of ULF/ELF broadband emissions (19:14–19:27 UT) during a southern oval crossing by S/C 3 of the CLUSTER flotilla. See text for explanations.

Here, $\rho_s = c_s/\Omega_i$ is the ion-acoustic gyro-radius, and $\lambda_e = c/\omega_{pe}$ is the electron inertia length (or skin depth). In this formalism the $\delta E/\delta B$-ratio becomes

$$\frac{\delta E}{\delta B} = V_A \cdot \sqrt{\left(1 + k_\perp^2 \rho_s^2\right)\left(1 + k_\perp^2 \lambda_e^2\right)} \quad (2)$$

Therefore, since the electron inertia length ($\lambda_e \approx 8-24$ km) is comparable to the ion gyro-radius ($\rho_H \approx 9$ km, $\rho_O \approx 36$ km), an increase in the $\delta E/\delta B$-ratio is expected for perpendicular wavelengths close to these two parameters. The ion composition varies during the event, and the O^+ content is about 10–60% of the total ion number density. The local cyclotron frequencies are close to 7.4–7.6 Hz (H^+) and 0.46 Hz (O^+). Doppler broadening ($\omega = |\omega_0 + \boldsymbol{k}\cdot\mathbf{v}|$) is relatively small due to the large scales involved. For example, during most of the period of the broadband emissions the spacecraft velocity relative the plasma was clearly below 3 km/s, as derived from the radial electric field component. Occasional peaks up to 9 km/s existed. If we assume the wavelength to be equal the smallest ion gyro-radius value of 9 km for ρ_H, then a maximum Doppler broadening of below 0.05 Hz would result for $k_\perp \rho_i = 1$.

[7] We carried out a quantitative fit to the $\delta E/\delta B$-ratio for the active broadband period using (1) and (2) and including possible Doppler broadening effects (Figure 2, panel c, red). The two different fits correspond to an H^+ and an O^+ dominated plasma respectively. A good fit could be produced for $k_\perp/k_\parallel = 800$ if we assume a wave solution with the $\boldsymbol{k}_\perp$-vector perpendicular to the plasma ram direction. In order to gain an almost equally good fit for the case when we assume that spatial plasma structures hits

the spacecraft with a velocity of 3 km/s, required $k_\perp/k_\parallel = 5000$. In that case the parallel wavelength had to be comparable to the size of the Earth's magnetosphere.

[8] We therefore conclude that the observed $\delta E/\delta B$-ratio increase with frequency can be interpreted in terms of a DAW for finite ω_0 and $\boldsymbol{k}$, i.e. in terms of waves. Even though we cannot completely exclude that Doppler-broadened spatial structures ($\omega_0 = 0$) dominate the broadband spectra by using extreme values, we found that a DAW with finite ω_0 easier explains the data.

[9] The Poynting flux (Figure 1, panels f and g) of the broadband emissions is directed toward Earth for this southern hemispheric crossing, and has been found pointing toward Earth for all the events in this study (Table 1). Also, the magnitudes (0.1–4 mW/m^2) correspond to typical observed energy fluxes in the topside ionosphere (1–100 mW/m^2) as well as with studies carried out based on FREJA and POLAR data [Volverk et al., 1996; Keiling et al., 2002].
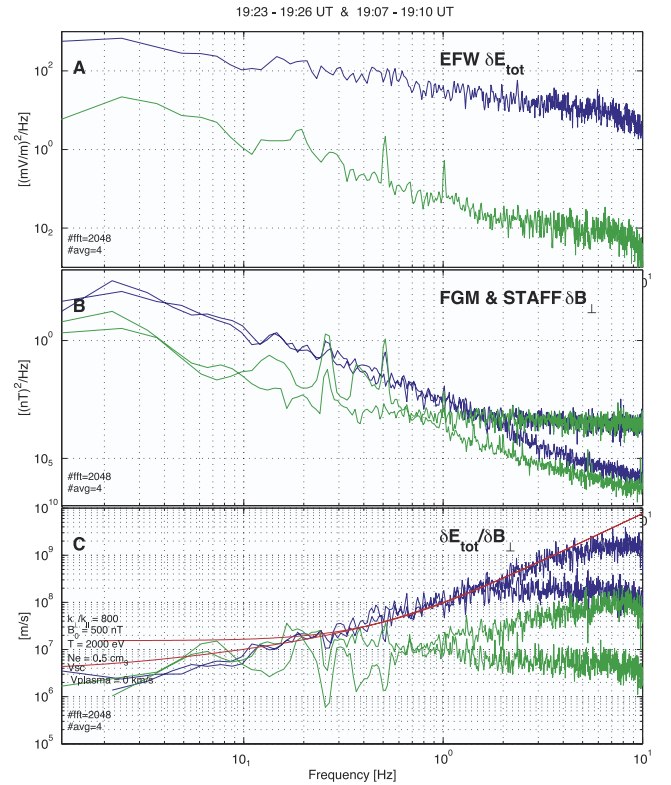

Figure 2. The E- and B-field power spectral densities (panel a and b) and the $\delta E/\delta B$-ratio (panel c) from a "broadband quiet" period (green, 19:00–19:07 UT) and from a "broadband active" region (blue, 19:20–19:27 UT). The two sets of magnetic data correspond to STAFF and high resolution FGM data respectively. The narrow electric and magnetic spikes at 0.25 Hz, 0.5 Hz and 1 Hz are due to the spinning spacecraft. The broader magnetic field peaks near 0.35 Hz and 0.15 Hz are similarly the rest of the STAFF antenna noise level after de-spinning and exist during the whole displayed interval (see Figure 1, panel b). The high resolution FGM data reaches the detection threshold above about 1 Hz, causing an artificial flat spectral behaviour.

Table 1. Event Characteristics Used in This Study. All Events are From Year 2001. Poynting Flux Values are Max Average Values (Over 250 Data Points) Based on Both STAFF and High Resolution FGM Magnetic Data

Date, UT Month	Max $S_{P,tot}$ [mW/m^2]	n_e [cm^{-3}] b	Ellipticity
Jan-14, ~04:30, N	0.3	0.05 − 0.5	Linear
Feb-14, ~01:00, S	0.2	0.2 − 2	Linear
Feb-26, ~00:30, N	4	0.1 − 2	Linear
Mar-19, ~08:30, S	0.1	0.1 − 10	Linear
Mar-19, ~11:30, N	0.1	0.05 − 5	Linear/Slightly RH
Mar-31, ~08:30, N	1.5	50 − 200	Linear/Slightly RH
Apr-28, ~19:20, S	0.3	0.03 − 0.3	Linear/Slightly RH
Apr-28, ~22:00, N	0.3	0.1 − 5	Linear

[10] The large-scale spatial-temporal evolution of the broadband emissions (**E**-field component) as inferred from the passage at different times by the four CLUSTER spacecraft, and the dependence on plasma density can be viewed in Figure 3. S/C 1 (Figure 3, panel a and b) enters the region of broadband waves first, followed by S/C 2 (panel c and d) and S/C 3 (panel e and f) at about the same time, and S/C 4 enters the region last (panel g and h). All the spacecraft enters the region of broadband emission near $71.6° − 71.8°$ indicating a spatial latitudinal boundary.

[11] From Figures 3 and 4 it is clear that the region of electric broadband emissions widens considerably equatorward during the time of the passage of the four CLUSTER spacecraft. This is not due to the slow convective movement of the existing broadband region, but instead due to the "sudden" appearance of a new region of broadband emissions at the edge of the already existing one. For instance, the new region detected by S/C 4 near 19:30 UT (panel g) corresponds to a new latitudinal region between $69.7° −$ $68.8°$ and is associated with a significant decrease in density in this region (panel h, compare with panels d and f), not that this region has drifted equator-ward. The new region is therefore a result of a temporal change. Since the Poynting flux was downward, this suggests a change in physical conditions in the source region above the CLUSTER spacecraft. Further evidence for this is given in the PEACE electron data (Figure 4, field-aligned components), where the plasma sheet electrons with energies near 800 eV, detectable by S/C 2 and 3 (panel b and c), disappear near 19:30 UT as measured by S/C 4 (panel d). It is this hot-electron plasma sheet boundary that limits equator-ward the region of the broadband emissions.

[12] From Figure 1, panel e, we can note that a slowly evolving electrostatic potential structure [e.g., *Mozer et al.*, 1977] occur in the region of broadband emissions near 19:17 UT (S/C 3) with an amplitude of about 150 mV/m p-p. This electric structure appear in S/C 1 near 19:15 UT (Figure 3, panels a and b) where the broadband emissions are as most intense at a sharp density gradient [see also *Vaivads et al.*, 2003]. Also, the event reported by *Marklund et al.* [2001] is associated with both intense broadband emissions as well as a sharp density gradient. The relationship between the emergence of electrostatic potential drops near density gradients where intensified broadband emissions exist may suggest that the intensification of the broadband wave generation may initialise the growth of such electric potential layers [see also *Wahlund et al.*, 1994].
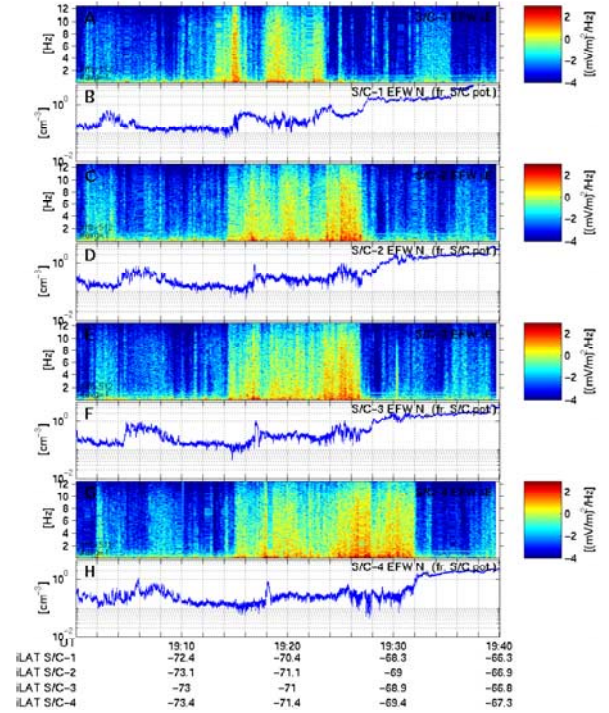

Figure 3. The E-field power spectral densities and electron densities from all four CLUSTER spacecraft. The region of broadband emissions widens equator-ward during a sub-storm growth phase.

[13] The most intense broadband emissions as detected by S/C 1 appear near sharp density gradients (e.g., 19:15 UT and 19:23 UT in Figure 3, panel a and b). This is a common feature among the other events studied. Another feature is that the density cavity widens when the broadband emission widens toward the equator, i.e., a large-scale
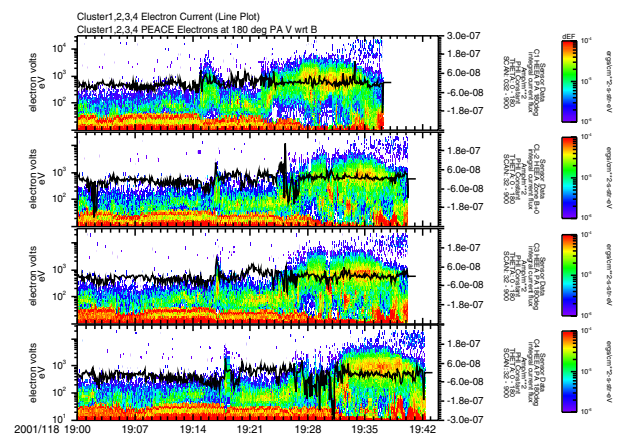

Figure 4. PEACE field-aligned earthward electron data from the four CLUSTER spacecraft together with field-aligned current density values (superposed black line). Except for the inverted-V acceleration near 19:15 − 19:19 UT, the broadband emissions are associated with ~80 eV electrons at the edge of the plasma sheet electrons (starting near 19:27 − 19:32 UT).

density cavity is formed. The ion spectrometer data show significant H^+ and O^+ outflows with energies around 1 keV simultaneous with the broadband emissions. Down-going electrons around 80 eV and up-going electron bursts up to of ~1 keV is detected within the region of broadband emissions [*Vaivads et al.*, 2003].

[14] Last we list the polarisation properties, as inferred from a method by *Carozzi et al.* [2001] by using the electric field components in the spacecraft spin plane. The results for the whole study are summarised in Table 1, where it is found that the ULF/ELF emissions are linear to slightly elliptically polarised for the whole measured frequency range. This fact supports the interpretation that the lower frequency electromagnetic emissions (propagating Alfvén waves) have the same origin as the higher frequency short-wavelength (locally damped) electrostatic emissions.

3. Conclusion

[15] We have shown that auroral broadband ULF/ELF emissions at CLUSTER distances $(4-5\ R_E)$ resemble broadband emissions observed at lower altitudes. For instance, compare the event, as presented here, with Plates 1, 2 and 3 in *Wahlund et al.* [1998] of FREJA observations at an altitude of 1700 km and even Figure 8 in *Wahlund et al.* [1993] with respect to EISCAT ground-based observations in the ionosphere. Note the similar sizes (few hundred km) of the large-scale regions of broadband activity and decreased plasma densities at the edge of the plasma sheet electron region.

[16] Intermittent auroral arc features occur within this larger scale region. The multi-spacecraft measurements by CLUSTER here show the temporal development of sharp density gradients and intensified broadband waves together with the formation of electric potential structures and particle acceleration within the larger scale density cavity. Indeed, there exist theoretical studies suggesting that Alfvénic activity can create parallel electric field structures on the edges of density cavities [*Génot et al.*, 2001].

[17] The detailed dispersion characteristics of the broadband waves as observed by CLUSTER and e.g. FREJA are also similar. We therefore believe that the broadband emissions observed by CLUSTER in the auroral region are consistent with dispersed linear polarised Alfvén waves (DAW) transporting energy downward to the ionosphere guided by the magnetic field lines. These waves are therefore an important aspect for the energy transport for the auroral processes leading to particle acceleration when dissipating part or all their energy along the propagation path by wave-particle coupling, causing ion heating, supra-thermal electron bursts and higher frequency ion-mode waves and possibly also electric potential structures.

References

Boehm, M. H., et al., High-resolution sounding rocket observations of large-amplitude Alfvén waves, *J. Geophys. Res.*, *95*, 12,157, 1990.

Bonnell, J., et al., Interferometric determination of broadband ELF wave phase velocity within a region of transverse auroral ion acceleration, *Geophys. Res. Lett.*, *23*, 3297, 1996.

Carozzi, T. D., et al., Full polarimetry measurements of SEE. First results, *J. Geophys. Res.*, *106*, 21,367, 2001.

Chmyrev, V. M., et al., Non-linear Alfvén wave generator of auroral particles and ELF/VLF waves, *Planet Space Sci.*, *37*, 749, 1989.

Escoubet, C. P., C. T. Russel, and R. Schmidt, The Cluster and Phoenix Missions, *Space Sci. Rev.*, *79*, 1–658, 1997.

Génot, V., P. Louarn, and F. Mottez, Fast evolving spatial structure of auroral parallel electric fields, *J. Geophys. Res.*, *106*, 29,633, 2001.

Gurnett, D. A., and L. A. Frank, A region of intense plasma wave turbulence on auroral field lines, *J. Geophys. Res.*, *82*, 1031, 1977.

Keiling, A., et al., Correlation of Alfvén wave Poynting flux in the plasma at $4-7\ R_E$ with ionospheric electron energy flux, *J. Geophys. Res.*, *107*, SMP24, 2002.

Louarn, P., et al., Observations of kinetic Alfvén waves by the Freja satellite, *Geophys. Res. Lett.*, *21*, 1847, 1994.

Lysak, R. L., and W. Lotko, On the kinetic dispersion relation for shear Alfvén waves, *J. Geophys. Res.*, *101*, 5085, 1996.

Marklund, G. T., et al., Temporal evolution of the electric field accelerating electrons away from the auroral ionosphere, *Nature*, *414*, 724, 2001.

Mozer, F. S., et al., Observations of paired electrostatic shocks in the polar magnetosphere, *Phys. Rev. Lett.*, *38*, 292, 1977.

Seyler, C. E., and K. Wu, Instability at the electron inertial scale, *J. Geophys. Res.*, *106*, 21,623, 2001.

Shukla, P. K., and L. Stenflo, Generalized dispersive Alfvén waves, *J. Plasma Phys.*, *64*(2), 125, 2000.

Stasiewicz, K., et al., Small scale Alfvénic structure in the aurora, *Space Sci. Rev.*, *92*, 423, 2000.

Vaivads, A., et al., Auroral acceleration: case study of Cluster/DMSP conjunction, *Geophys. Res. Lett.*, *30*, 1106, 2003.

Volverk, M., et al., Solitary kinetic Alfvén waves: A study of the Poynting flux, *J. Geophys. Res.*, *101*, 13,335, 1996.

Wahlund, J.-E., et al., Electron energization in the topside auroral ionosphere: on the importance of ion-acoustic turbulence, *J. Atmos. Terr. Phys.*, *55*, 623, 1993.

Wahlund, J.-E., et al., On ion acoustic turbulence and the nonlinear evolution of kinetic Alfvén waves in aurora, *Geophys. Res. Lett.*, *21*, 1831, 1994.

Wahlund, J.-E., et al., Broadband ELF plasma emission during auroral energization 1. Slow ion acoustic waves, *J. Geophys. Res.*, *103*, 4343, 1998.

————————————

J.-E. Wahlund, A. Vaivads, M. André, M. Backrud, S. Buchert, A. I. Eriksson, G. Gustafsson, D. Sundkvist, and A. Tjulin, Swedish Institute of Space Physics, Uppsala Division, P.O. Box 537, SE-751 21 Uppsala, Sweden. (jwe@irfu.se; andris@irfu.se; ma@irfu.se; marie@irfu.se; sb@irfu.se; aie@irfu.se; gg@irfu.se; davids@irfu.se; at@irfu.se)

A. Yilmaz, Dept. of Physics, Çanakkale Onsekiz Mart University, Çanakkale, Turkey. (akriaw@yahoo.com)

A. Balogh and M. Dunlop, Space and Atmospheric Physics Group, The Blackett Laboratory, Imperial College, Prince Consort Road, London SW7 2BW, UK. (a.balogh@ic.ac.uk; m.dunlop@ic.ac.uk)

J. Bonnell, Space Science Laboratory (SSL), University of California, Berkeley, USA. (jbonnell@ssl.berkeley)

T. Carozzi, Space Science Centre., University of Sussex, Brighton, E. Sussex, BN1 9QT, UK. (T.Carozzi@sussex.ac.uk)

N. Cornilleau and P. Robert, CETP/CNRS, University of Versailles Saint Quentin, 10-12 Av. De l'Europe, 78140 Vélizy, France. (nicole.cornilleau@cetp.ipsl.fr; patrick.robert@cetp.ipsl.fr)

M. Parrot, LPCE/CNRS, 3A Avenue de la Recherche Scientifique, 45071 Orléans Cedex 2, France. (mparrot@cnrs-orleans.fr)

A. Fazakerley, Mullard Space Science Laboratory, University College London, Holmbury St. Mary Dorking, Surrey, RH5 6NT, UK. (anf@mssl.ucl.ac.uk)

D. Winningham, Southwest Research Institute, P.O. Drawer 28510, San Antonio, TX 78228, USA. (dwinningham@swri.edu)